

Monte Carlo Evaluation of the Feynman Path Integral to Determine Wavefunctions Within Quantum Anisotropic Potentials

D.M.Caro

L3 Computing Project - The Feynman Path Integral
Submitted: March 15, 2024, Date of Experiment: March 8, 2024

A study into the Feynman Path Integral, developed by Richard Feynman, with numerical evaluation of the propagator within various quantum potential wells through the use of a Markov Chain Monte Carlo (MCMC) algorithm named the Metropolis-Hastings algorithm. This has been used to determine the properties of non-analytic ground state wavefunctions of the Harmonic and Higgs potentials, as well as a custom made anisotropic potential. This includes the probability density functions (PDF) and the excitation energy to the first excited state. The PDF's for these potentials were determined with great success, whereas the excitation energy provided varying results. An analysis on the accuracy, applications and limitations of this method were then conducted. The path integral was initially developed as an alternative formulation for quantum mechanics to determine the time evolution of a wavefunction. The path integral provided a link between classical and quantum physics previously unrecognised by Schroedinger's and Heisenberg's respective formulations. It has since provided an important foundation in modern quantum mechanics, allowing for the development of quantum electrodynamics, quantum field theory and ultimately the standard model of particle physics.

I. Introduction & Theory

A. The Propagator

During the 1940s Richard Feynman formulated his path integral for non-relativistic quantum mechanics, releasing it in his article in the journal 'Reviews of Modern Physics', 1948 [1]. This built upon the previous work of Norbert Wiener, who developed the 'Wiener process' that describes continuous, time varying, stochastic processes; and Paul Dirac [10], who motivated the idea of a quantum mechanical Lagrangian. Feynman sought to create this formulation to bring a closer link between classical and quantum physics. The work would find a new approach to describe the propagation of a wavefunction through space-time, by applying the classical Lagrangian to quantum particles, through Hamilton's principle of least action. The path integral itself is given by the equation [8],

$$\Psi(x_b, t_b) = \int G(x_b, t_b; x_a, t_a) \Psi(x_a, t_a) dx_a \quad (1)$$

Where, Ψ is the wavefunction at either the space-time points $A = (x_a, t_a)$ or $B = (x_b, t_b)$ and $G = G(B; A)$ is the propagator between these points. The integral provides a new wavefunction equivalent to those gained by the differential equations of Schroedinger and matrix algebra of Heisenberg. The link to Schroedinger can be seen from investigating the equation for the time dependent wavefunction. The wavefunction, given by time evolution unitary operator, $U = e^{-\frac{i}{\hbar} \hat{H}t}$, is $\Psi(x, t) = U(t)\psi(x, 0)$ [2]. In Feynman's formulation the propagator, also known as the 'Feynman kernel' [11] is an integral formulation of U . Where the probability of each possible path between the two space time points A and B , given by G , has been integrated over all of space time to arrive at the final, time evolved, wavefunction. The propagator is thus the transition amplitude between two wavefunctions which, in natural units ($\hbar = 1$), is given by,

$$\langle x_a, t_a | x_b, t_b \rangle = \left\langle x_a | e^{-i\hat{H}(t_b-t_a)} | x_b \right\rangle = \int \mathcal{D}x(t) e^{iS[x(t)]dx} \quad (2)$$

Where, \hat{H} is the Hamiltonian of the system, S is the action of a single path and \mathcal{D} denotes an integral over all paths $x(t)$. Subsequently, as this is an integral over all possible paths, we can express the propagator in its summation form as an infinite weighted sum of each path [11],

$$G(B, A) = \sum_{\text{paths}}^{\infty} e^{\frac{i}{\hbar} S_p[B, A]} \quad (3)$$

Where, $S_p[B; A]$ is the action of a path between A and B and provides a weighting equivalent to its probability. Evaluating the integral in Eq.(2) for the action of a free particle in imaginary time (through a Wick rotation), the propagator can be shown to be a Gaussian distribution [11]. This illustrates a important concept of the integral Eq.(1): it is a form of Huygens' wavelet principle [6], where every point on the wavefront of $\Psi(x_a, t_a)$ emits a Gaussian wave. This is of important relevance when observing the shapes of the probability density functions in this paper.

B. Markov Chain Monte Carlo

Monte Carlo methods are used in a broad range of algorithms that employ random numbers to solve problems which may be deterministic in nature. Here it is used for numerical integration. The fundamental principal requires random numbers to scan an interval $[x_i, x_f]$, with their locations, x_{MC} , equating to a value of the function $f(x_{MC})$. A collection of these values are then used to numerically approximate the integral once the number of samples (x_{MC}) increases to a sufficient amount. The efficiency can be improved when we consider sampling the variable x according to a weighting $w(x)$ corresponding to a normalised probability density function. The integral is now evaluated

through the equation [5], where $f(x)$ is our function and N is the number of samples,

$$I = \int_{x_i}^{x_f} w(x)f(x)dx \simeq \frac{1}{N} \sum_{r=1}^N f(x_r) \quad (4)$$

Markov chains are consolidated into this method due to their use in modelling stochastic processes. The definition for a chains is simple: it is a sequence of random states, X_i , where the probability of moving to the next state, X_{i+1} , depends only on the present state, known as the Markov property. The extension of the Monte Carlo method is hence as expected; instead of a sampling a multi-dimensional region uniformly, each site, \underline{x}_i , is visited in the space from a previous site, \underline{x}_{i-1} , with a probability proportional to a given distribution function $\pi(\underline{x})$ [5] (not requiring normalisation to unity).

Thus, in a Markov chain Monte Carlo (MCMC) algorithm, samples are generated preferentially where $\pi(\underline{x})$ is large. The points in these chains are locally correlated (\underline{x}_i depends only on \underline{x}_{i-1}) and ergodic (all parts of a space will be visited). Each point \underline{x}_i is picked from the previous point \underline{x}_{i-1} by a transition probability function of the two variables, given by $P_i = p(\underline{x}_i|\underline{x}_{i-1})$ and can approach the target distribution $\pi(\underline{x})$, once enough samples are generated [3]. The Metropolis Hastings algorithm provides a general framework for MCMC to obtain a chain of random samples proportional to a probability distribution, where in our instance: $P_i = G \propto e^{\frac{i}{\hbar} S[\underline{x}]}$ and $\pi(\underline{x}) \propto |\phi(\underline{x})|^2$.

C. Potential Wells

Ultimately, the aim of the code was to correctly determine the properties of wavefunctions within various quantum potential wells. In this paper the potentials investigated are: the harmonic potential, Higgs potential and an arbitrary anisotropic potential. The harmonic potential, and the quantum harmonic oscillator it describes, is a key potential used in quantum mechanics and condensed matter physics. In part due to its simplicity, but specifically in its application of approximating smooth potentials near a stable equilibrium point - such as an ion. The function, as described in 2-dimensions, is;

$$V(\underline{x}) = \frac{1}{2}m\omega^2 r^2 \quad (5)$$

Where, $\underline{x} = (x, y)$ describes two orthogonal spatial dimensions; m the mass of the particle; $\omega = \sqrt{\frac{k}{m}}$ the frequency of the particle and $r = \sqrt{x^2 + y^2}$ the distance from the origin, for simplicity we shall set, $m = 1$. The wavefunction's PDF, which will not be derived here, can be found most simply through solving the time-independent Schrödinger equation, $\hat{H}\psi = E\psi$, and applying the Born rule. The groundstate solution is given as [12],

$$P(\underline{x}) = |\psi_0(\underline{x})|^2 = \left(\frac{m\omega}{\pi\hbar} \right) e^{-\frac{m\omega}{\hbar} r^2} = \frac{\omega e^{-\omega r^2}}{\pi} \quad (6)$$

$$E_{n_1, n_2} = \hbar\omega[(n_1 + n_2) + 1] \implies \Delta E = E_{1,0} - E_{0,0} = \omega \quad (7)$$

Where on the last line we have also used natural units. It is of interest to note that, similarly to the propagator, the PDF has a Gaussian form.

The Higgs potential is the potential of the Higgs boson, which itself is responsible for producing the mass of the elementary particles, W^\pm and Z^0 bosons, through the Higgs mechanism. This occurs due to the symmetry breaking of the Lagrangian in the electroweak local gauges $SU(2)_L \times U(1)_Y$, sometime after the Big Bang. The new complex scalar field has a circular lowest energy state, instead of the singular minima before symmetry breaking. From a consequence of the weak gauge, these particles are excited in the radial direction of the potential; providing a change in value of their potential energy and giving rise to their mass. The potential of this mechanism is hence given as [14],

$$V(\phi) = \frac{1}{2}\mu^2\phi^2 + \frac{1}{4}\lambda^4\phi^4 \quad (8)$$

Where, ϕ is a complex scalar field, but here treated as a position $\underline{x} = (x, y)$. In this paper μ and λ are used as arbitrary constants, given as $\mu = 2$ and $\lambda = 1$, subsequently forming a minima at a position $\nu = \frac{\mu}{\lambda} = 2$ from the origin. Finally the anisotropic potential investigated in this paper is given as,

$$V(x, y) = \cos 2x + \cos 2y + Ae^{r^2} \quad (9)$$

Where, $A = \frac{1}{5000}$ is the constant that determines when the exponentials become the dominant terms in the function. This constant allows for a width of the potential as approximately $-3 < x < 3$, which is of a similar scale as the previous potentials. The trigonometric functions produce symmetric periodic minima for the particle, while the exponentials act as the 'walls' of the potential.

II. Methods

A. Discretisation

In order to apply the path integral to the Metropolis-Hastings algorithm, we must find a discretised form of the integral of which we can numerically evaluate. To do this, we must first perform what is known as a Wick rotation, where we use imaginary time $t \rightarrow -i\tau$, such that we are now performing a Euclidean integral (integrating over a real domain). We then set the path to be circular such that $x_a = x_b = x$ and finally define a total time $T = \tau_b - \tau_a$. Again we are using natural units, and are hence left with the propagator given as,

$$G = \langle x|e^{-\hat{H}T}|x\rangle = \sum_n \langle x|\psi_n\rangle e^{-E_n T} \langle \psi_n|x\rangle \quad (10)$$

Where, n is an energy level, ψ_n is an eigenstate and we have substituted the eigenvalue E_n for the Hamiltonian, while also using the completeness relation, $\sum_n |n\rangle\langle n| = 1$. When T is large the sum is dominated by the lowest energy state, hence ψ_0 'condenses' out of the summation and we are left with the equation,

$$\langle x|e^{-\hat{H}T}|x\rangle \rightarrow e^{-E_0 T} |\langle x|\psi_0\rangle|^2 \quad (11)$$

Thus, we are limited to determining the PDF of only the groundstate wavefunction in a potential well. We can extract the energy difference between the ground and first excited state by interrupting the propagation of the ground-state through introducing new operators. If we take the mean of two arbitrary positions in the path, $x(t'_1) = x'_1$, $x(t'_2) = x'_2$, we have the equation;

$$\langle\langle x'_1 x'_2 \rangle\rangle = \frac{\int D x'_1 x'_2 x(t) e^{-S[x]}}{\int D x(t) e^{-S[x]}} \approx \frac{1}{N_{CF}} \sum_{\alpha=1}^{N_{CF}} G[x^\alpha] \quad (12)$$

Where, x^α is a path out of the set $\{x^\alpha\}_{\alpha=1}^{N_{CF}}$. Where the last line is the computational evaluation of the integral using the Monte Carlo approximation, Eq.(4), with a large number of paths N_{CF} . Repeating a similar derivation as earlier we get,

$$G(t) = \langle\langle x'_1 x'_2 \rangle\rangle \rightarrow e^{-(E_1 - E_0)\tau} |\langle \psi_0 | \tilde{x} | \psi_1 \rangle|^2 \quad (13)$$

Where, \tilde{x} is an arbitrary position in a path. Hence, we arrive at the energy difference, where a is the time step and forms the set, $\{\Delta E_j\}_1^{n-1}$;

$$\log \left(\frac{G(t)}{G(t+a)} \right) \cdot \frac{1}{a} \rightarrow E_1 - E_0 = \Delta E \quad (14)$$

B. Metropolis-Hastings Algorithm

Before applying the Metropolis algorithm we must also define a path, x^α (as mentioned previously), as a discrete set of temporal lattice points, n , with a spatial position associated with it. Such that, $x^\alpha = \{x_0, \dots, x_n\}$, so that we may form a total configuration of paths, given as the set $\{x^\alpha\}_{\alpha=1}^{N_{CF}}$. The total time given for this path is T , and hence the time step between each point is $a = \frac{T}{n-1}$. The Metropolis algorithm then provides the framework of the instructions for our code to generate the N_{CF} number of paths, which in this case is:

1. Initialise the algorithm by inputting a path x^α
2. Generate a random deviation, δx , within the limit $|\delta x| \leq \epsilon$ and perturb the first point in the path x_0^α
3. Calculate the change in action ΔS of this new path
4. Retain the new point if either:
 - $\Delta S < 0$
 - $r < e^{-\Delta S}$, where $\Delta S \geq 0$ and r is a random number between $0 \leq r \leq 1$
5. If neither of these conditions are met, keep the initial path
6. Inspect the next point in the path, x_1^α by repeating from step 2.
7. Repeat 2. - 6. until all n points from the initial path are inspected (called an update) and save this path

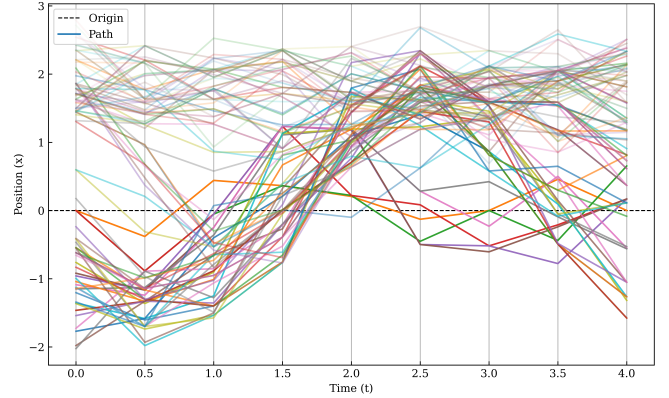


FIG. 1: A plot of $N_{CF} = 5 \cdot N_{cor}$ paths, with $T = 4$ and $n = 9$ lattice points. Produced from the Metropolis algorithm in a 1D Higgs potential. The alpha of each path has been gradually reduced in order to more easily visualise the continuity of the path.

In order to correctly apply this algorithm, there are a few additional remarks. Firstly ϵ must be kept constant throughout the path generation, and must be adjusted such that each point has a $40 - 60\%$ chance of being changed each update. Then, before the paths can begin to be saved into an array, the atypical initialising path of $x^0 = \{0_0, \dots, 0_n\}$, must first be thermalised within the potential. This equates to updating the initialising path $5 \cdot N_{cor}$ [7] number of times. Where the value N_{cor} is the correlation relation of our algorithm, which arises as consecutive paths may be highly correlated, with $N_{cor} \propto \frac{1}{a^2}$. The Metropolis algorithm can now be applied to this thermalised initialising path, but, again due to the correlation of paths, we must update the path N_{cor} number of times before saving it to our array. We continue this until N_{CF} total paths are made, which can adequately resolve the probability density function. Thus, ultimately $N_{cor} \cdot N_{CF}$ number of updates are applied to the initial path, which must be taken into consideration for the running time of the algorithm.

The energy of the particle at the current point, x_j , is calculated discretely with the equation,

$$E_{tot} = \sum_{j=0}^{n-1} \frac{1}{2m} \left(\frac{x_j (x_j - x_{j+1} - x_{j-1})}{a} \right)^2 + V\left(\frac{x_j}{2}\right) \quad (15)$$

Where the action is $S = a \cdot E$. Note the form of the kinetic energy term (which is derived from the improved action), that the summation is local (i.e only involving adjacent points) and that j is calculated as $j \bmod(n)$ such that a loop is maintained in the path. The extension to another dimension is subsequently fairly straightforward; here a path in the new dimension, y^α , must be seeded for the algorithm in the same way as x^α and sampled with the same regularity as the x_j^α 's. The new perturbed paths, corresponding to a series of coordinates in our space \underline{x}_j^α 's, are fed into the functional for the action. In two-dimensions the total energy is expressed as,

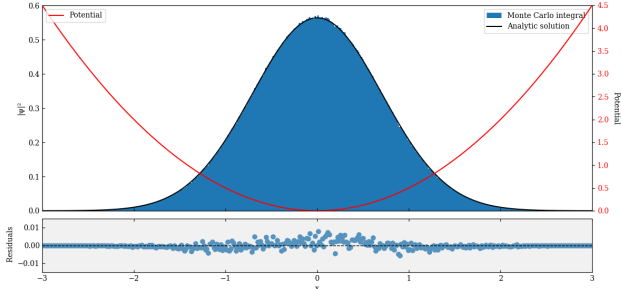
$$E_{tot} = \frac{1}{2} m |\underline{v}|^2 + V(x, y) = KE_x + KE_y + V(x, y) \quad (16)$$

Where, the KE_x and KE_y terms of the kinetic energy can be calculated using the summation shown for the 1D case. The action of the paths is then calculated as previously shown and new positions are either collectively accepted or rejected based on the acceptance criteria of the algorithm.

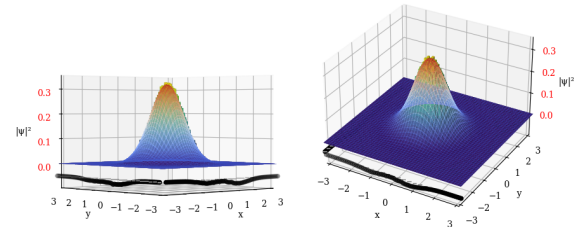
III. Results

A. Harmonic Potential

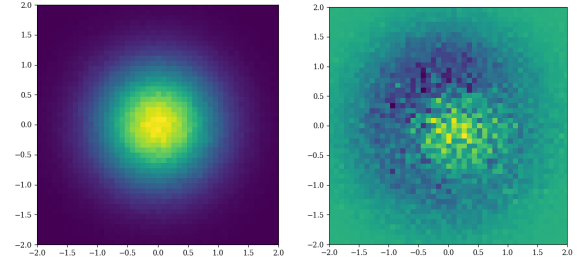
Preliminary results from the Metropolis algorithm applied to a harmonic potential, with a known analytic solution are shown below. The one-dimensional harmonic potential was the first to be investigated to verify that the Metropolis and ΔE code were working appropriately. The relevant potential and PDF are seen in Eq.(5) and Eq.(6), when $y = 0$.



(a) A histogram of points produced from the Metropolis algorithm in a 1D harmonic potential, as given in Eq.(5) where $y = 0$, with one million paths generated. The potential itself is plotted on the same axis to visually see the position of the minimum, with the unnormalised residuals plotted below it.



(a) The front and side on views of the 3D histogram from the 2D harmonic potential, as given in Eq.(5), for $N_{CF} = 10^5$ (per axes). The analytic solution is overlaid on the histogram to show the accuracy of the plot. The unnormalised residuals have been average over x and y and have been enlarged to show trends in the data.



(b) The 2D contour plot of the (c) The 2D contour plot of the histogram to visualise the distribution of the PDF. (d) The ΔE of a 2D harmonic potential, with $\omega = 1$, $\Delta E(t_0) = 0.98991$.

FIG. 3: Results for the 2D harmonic potential.

B. Higgs Potential

The results from the Higgs potential, given in Eq.(8) with $\mu = 2, \lambda = 1$, is seen below in Fig.4. The PDF was plotted with good accuracy with the count being equally distributed around the ring.

C. Anisotropic Potential

The results from the anisotropic potential, given by Eq.(9) with $A = \frac{1}{5000}$, are seen below in Fig.5. Each of the four minima were discovered by the algorithm well with an equal distribution of counts between each of them, as was expected.

IV. Discussion

A. Accuracy

As seen in Fig.2, the algorithm was able to accurately determine the probability density and excitation energy of

The results, displayed as a 3D histogram and contour plots, of the extension of the Metropolis algorithm to the 2-dimensional harmonic oscillator potential, seen in Eq.(5) is shown below in Fig.2. This was to confirm that the two-dimensional results of the PDF and ΔE were accurate.

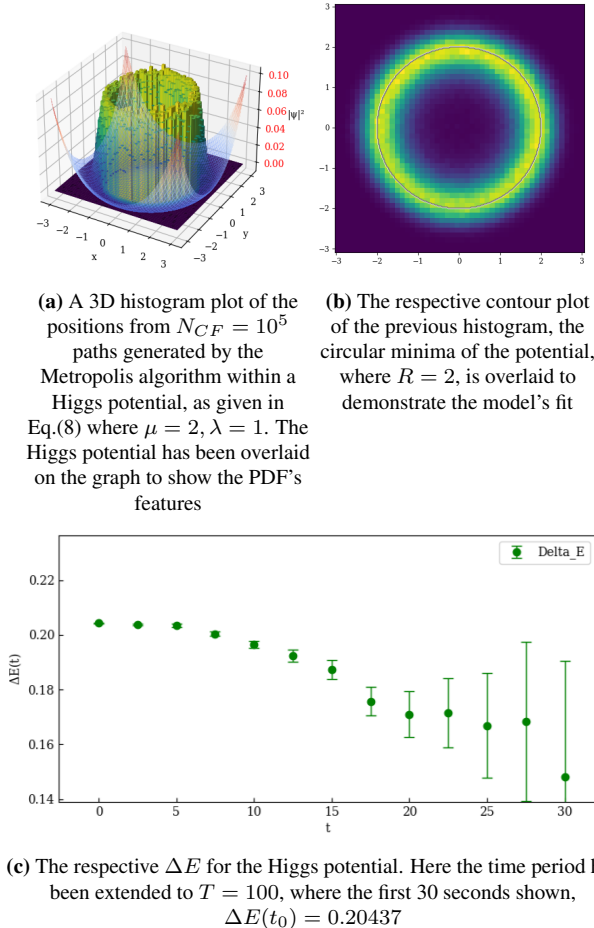


FIG. 4: Results for the Higgs potential.

a wavefunction for a 1D harmonic potential, once a sufficiently large number of paths had been generated. This can clearly be seen within the residuals as there is only a slight deviation from the analytic solution at the point where the function peaks. The lack of accuracy at this location, compared to the edges, can be understood as a consequence of the higher population rate for the central region, creating larger discrepancies between adjacent points. The calculation for the excitation energy produces an accurate result for the first few seconds of the graph. After this point, however, it can be seen to quickly, and randomly, diverge. The result for a harmonic potential where $\omega = 2$ produces a less accurate result, with the analytic solution lying outside of the error bars. Similarly, this result erratically diverges from the asymptote, but now more quickly than before. However it can still be seen as a reasonable approximation of the theoretical value.

Once the algorithm was extended into 2-dimensions the harmonic oscillator was again used to check that the algorithm was working correctly. Fig.3(a) demonstrates the algorithm's exceptional model of the groundstate PDF within a 2D harmonic potential. Much like the 1D solution, the calculation lacks accuracy at the peak of the analytic solution, where the residuals, accentuated by three times ($3 \times R$), show deviation from the mean. The relation of the residuals can also be seen in the 2D colour mapping of Fig.3(c), where the largest deviations are seen at the peak. Again the excitation energy, Fig.3(d), was successfully calculated for the initial stages of the graph. However due to the fewer

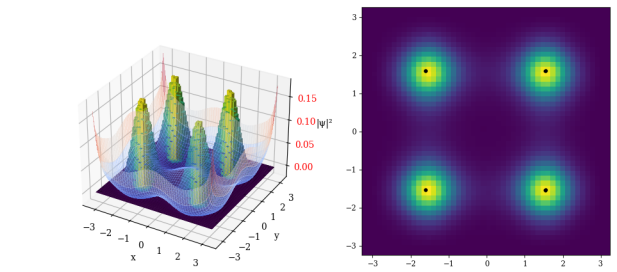


FIG. 5: Results for the anisotropic potential.

number of configurations that can be calculated in the 2D case, than in 1D for a similar computing time, the solution diverged much more quickly than before. A calculation for $\omega = 2$ was not performed as this was shown to be successful for the one-dimensional solution.

B. Numerical Solutions

After successful tests of the code the algorithm was applied to find the PDFs and ΔE s of potentials that are difficult, or impossible, to calculate analytically. As is the essence for developing the Metropolis algorithm.

Fig.4 shows the results of the Metropolis algorithm being applied to the Higgs potential, given by Eq.(8). This can be seen to describe the expected PDF successfully in Fig.4(b), where the histogram peaks along the circular minima of the function. The radius of this circle, given by $R = \frac{\mu}{\lambda}$, has a value of $R = 2$. Applying the code to determine the difference in energy between ground and first excited state appeared to be less successful. However a short asymptotic/constant relation in $\Delta E(t)$ can be seen for the initial stages of the graph, implying a reasonable value was estimated. Taking a similar approach to that of the harmonic potential, where it takes the most accurate solution at of ΔE at $t_0 = 0$, we can estimate that $\Delta E \approx 0.204$. However no literature was found to compare this value to. Interestingly, it seems that increasing the time period of the paths, while also increasing the deviation size, ϵ , such that the probability of a point change is $p \approx 40\%$ produces a more stable graph for the first initial values.

Finally applying the algorithm to a custom made potential, in this paper simply named an anisotropic potential, given by Eq.(9), and shown by Fig.5 provides some very

intriguing results. The 4 minima are of equal depth and distributed an equal distance from the origin, with the location of the minima shown by the black dots. Examining the contour plots of Fig.5(b), the minima of the potential wells were found exceptionally well. The algorithm also peaked well at all the minima, however it can be seen that they remain not entirely equal. A reason for the discrepancy while still taking a large number of samples, is that once in the well the algorithm struggles to leave. This is due to a combination of the Markov chain required by the algorithm meaning that the particle must follow a continuous path. While also only able to move between wells with a frequency relative to random number r , given in the Metropolis' instructions. As the random value that is chosen determines how often the particle is able to move to a more energetic path, in order for it to travel between minima. This frequency can, however, be increased via increasing the point deviation size, given by ϵ . Doing so can allow the path to move to more distant points, potentially allowing it to immediately fall inside a new well, allowing for the most frequent movement between minima.

C. Extension

Theoretically the energies of higher order wavefunctions can be extracted from the propagator [7] and with the option to easily apply it to more relevant 2D anisotropic potentials, the algorithm seems to be very capable for analysing potential wells. An interesting, and fairly trivial, extension is to more physically relevant 3-dimensional potential wells. This will, however, incur two obvious problems: firstly the visualisation of the PDF function in a 3D well; and secondly, the key issue, is the computing resources required to sufficiently detail the PDF. This is due to the run time increasing as $O(n^D)$, with D as the number of dimensions. This can be understood as the number of paths produced in each direction of a N-dimensional system, N_{CF} , determines the accuracy of the program and must be equal. In this paper I have determined that this value is 10^4 as a minimum bound. So the time complexity of the algorithm will increase exponentially, with the number of dimensions, x_i .

The Metropolis algorithm is, however, not limited to evaluating merely the properties of particles in potential wells. As discussed by both Lepage.P [7], Scott.J [13] and Matsufuru.H [9], the methods used here can be applied to Quantum Chromodynamics (QCD). The 1D temporal lattice is maintained with the potential being replaced by a scalar field. Points on a path are replaced by a 3×3 matrix while being perturbed by randomly generated SU_3 matrices. The QCD action cannot be directly discretized while maintaining relevant gauge invariances, so approximations must be made, such as the Wilson action [7]. This can be used to calculate the excitation's in the scalar field which refer to the production of gluons and quarks by calculating action loops, such as a Wilson loop.

D. Limitations

Within the entirety of the project it must be noted that higher order wavefunctions cannot be attained via this method. As seen in the theory, it is due to the form of the propagator being the summation of all wavefunctions.

Hence the only way to attain a singular one is to take the large time limit, allowing the groundstate to 'condense' out of the summation as the higher order wavefunctions become negligible terms. Also, though not explicitly stated in relevant literature, the evaluation of the propagator seems to be limited in its ability to calculate the excitation energy to the first excited state within different potentials. Though a constant value of the ΔE was achieved in Fig.4(c) and Fig.5(c), it was limited at best. A reason for this is difficult to establish as the theory uses a generalised action (hence one independent of potential). It may be due to a lack of paths generated or, as instability was seen to occur more quickly in the value of ΔE of the harmonic potential with $\omega = 2$; these more asymmetric potentials may create a faster and more accentuated deviation. Importantly however, with a lack of available literature to compare the values to, little conclusions can be made about the results.

The errors incurred within the code were difficult to evaluate. The goodness of fit from the Metropolis algorithm was partially described within the residuals of the 1D and 2D harmonic oscillators, seen in Fig.2 and Fig.3(a),(c), where there is a known analytical solution. However as they are unnormalised they provide a more qualitative assessment of the error. The errors of those in the potential wells without analytical solutions could, of course, not use this method. One way that was unfortunately not attempted here, due to time constraints, would be to run the Metropolis algorithm multiple times for the same potential. Finding a standard deviation and average between histogram counts throughout the run, while using standardised bin locations for all histograms.

V. Conclusions

Ultimately, this simple code was successful at numerically evaluating the probability density function of a groundstate wavefunction in anisotropic potential wells, as well as the excitation energy within the 1D and 2D harmonic potential. This was demonstrated by correct results seen in the PDF of the groundstate wavefunction of a particle in the harmonic and Higgs potentials, and the agreement of the experimental excitation energy to the analytical values. Extending this to the anisotropic potential, with no analytical solution, it is difficult to determine the accuracy of the results. No changes, of course, were made to the methodology, with the potential also being designed in order to avoid any potential errors in the algorithm - namely that the potential is 'closed', such that there are walls, and it contains a symmetry. Consequently, I have not found clear reasons as to why these plots could not be used as a predictive basis for the physical system.

Intrinsic limitations remain in the code of course. Such as the theory requiring an infinite number of paths for true accuracy, which is limited in practicality by more than just computational resources. As well as the inability to accurately determine all the properties of wavefunctions within a potential well, as the code is limited to evaluating the groundstate wavefunction. The code also appears to struggle with increasingly complex potentials that lack symmetries. The reliability of the results could also have been improved via repeat simulations, as mentioned in limitations, to provide a confidence level in the resultant, averaged, histograms.

References

- [1] Feynman, R.P. (1948). Space-Time Approach to Non-Relativistic Quantum Mechanics. *Reviews of Modern Physics*, 20(2), pp.367–387. doi:<https://doi.org/10.1103/revmodphys.20.367>.
- [2] Grosche, C. (1993). An Introduction into the Feynman Path Integral. [online] arXiv.org. doi:<https://doi.org/10.48550/arXiv.hep-th/9302097>.
- [3] Hastings, W.K. (1970). Monte Carlo sampling methods using Markov chains and their applications. *Biometrika*, 57(1), pp.97–109. doi:<https://doi.org/10.1093/biomet/57.1.97>.
- [4] I. G. Hughes and T. P. A. Hase, Measurements and their Uncertainties, Oxford University Press, Oxford, 2010.
- [5] Joseph, A. (2020). Markov Chain Monte Carlo Methods in Quantum Field Theories : A Modern Primer. [online] Cham, Switzerland: Springer International Publishing. Available at: <http://dx.doi.org/10.1007/978-3-030-46044-0> [Accessed 15 Mar. 2024].
- [6] Landau, R.H., José, M., Páez, M.J., Kowallik, H. and Jansen, H. (1997). Computational Physics. Wiley-VCH, pp.309–321.
- [7] Lepage, G.P. (2005). Lattice QCD for Novices. [online] arXiv.org. doi:<https://doi.org/10.48550/arXiv.hep-lat/0506036>.
- [8] MacKenzie, R. (2000). Path Integral Methods and Applications. [online] arXiv.org. doi:<https://doi.org/10.48550/arXiv.quant-ph/0004090>.
- [9] Matsufuru, H. (2007). Introduction to lattice QCD simulations. [online] Available at: https://research.kek.jp/people/matsufuru/Research/Docs/Lattice/Introduction/note_lattice_ver0.90.pdf [Accessed 13 Mar. 2024]. Ver.1.0.
- [10] P. A. M. Dirac (2005). The Lagragian in Quantum Mechanics. World Scientific eBooks, pp.111–119. doi:https://doi.org/10.1142/9789812567635_0003.
- [11] Perepelitsa, D. (2018). Path integrals in Physics. CRC Press eBooks. doi:<https://doi.org/10.1201/9781315273358-8>.
- [12] Rowe, G. (2021). Two-dimensional harmonic oscillator. [online] Physicspages.com. Available at: <https://physicspages.com/TOC>
- [13] Scott, J. (2016). OpenCommons@UConn Monte Carlo Applications and Lattice QCD. [online] Available at: https://digitalcommons.lib.uconn.edu/cgi/viewcontent.cgi?article=1502&context=srhonors_theses [Accessed 13 Mar. 2024].
- [14] Thomson, M. and Cambridge University Press (2018). Modern particle physics. Cambridge: Cambridge University Press, pp.460–475.

Error Appendix

The residuals for Fig.2. and Fig.3 were calculated as,

$$Res = y_{hist} - y_{mod} \quad (17)$$

where y_{hist} is the normalised height of a bin, y_{mod} is the analytic value of the PDF at the location of the centre of the bin.

The errors within Fig.2-Fig.5 were derived in reference to Lepage.P [7] as described in a 'bootstrap' method. A "bootstrap copy" is one that is made from the original set of propagator values, $\{G^\alpha\}_1^{N_{CF}}$, where random values of the propagator are taken from this set until a new set of the same size is formed, $\{G'^\alpha\}_1^{N_{CF}}$, allowing omissions and repetitions. In this paper 100 bootstrap copies are made for each ΔE calculation. New mean and standard deviation values of $\{\Delta E_j\}_1^{n-1}$ were calculated using these copies, with the standard deviation between values given by,

$$\sigma_{M-1} = \sqrt{\frac{\sum(F_i - \mu_F)^2}{M - 1}}, \quad (18)$$

Where M is the number of bootstrap copies formed, in this paper given as $M = 100$

All methods for error analysis is derived in reference from Hughes and Hase [11]

Scientific Summary for a General Audience

In this exploration of quantum mechanics, I employed the Metropolis algorithm to unravel the intricacies of the Feynman path integral—a revolutionary formulation introduced by Richard Feynman. This integral serves as a bridge between classical and quantum physics, encompassing all possible paths a particle could take. Specifically, my investigation honed in on calculating wavefunctions within 2D potential harmonic oscillators and the captivating Higgs potential, utilizing the Metropolis algorithm to determine the Probability Density Function (PDF) of these wavefunctions.

The methodology involved initializing the algorithm at the origin, generating random deviations within defined limits, and assessing changes in action. Notably, the algorithm retained new paths based on specific conditions, such as a negative change in action or a probability threshold. These efforts shed light on the energy disparities between ground and first excited states within confined systems, unraveling the nuanced behavior of wavefunctions. Importantly, the Metropolis algorithm parameters were meticulously chosen to ensure a comprehensive exploration of potential landscapes. In summary, this research contributes to a deeper understanding of quantum phenomena, providing valuable insights into the behavior of particles within potential wells.